

論文 / 著書情報
Article / Book Information

| | |
|------------------|---|
| Title | Selective Extraction and Hydrotreatment of Biocrude from Sewage Sludge: Toward High-Yield, Alkane-Rich, Low-Heteroatom Biofuels |
| Authors | Muhammad Usman, Shuo Cheng, Sasipa Boonyubol, Muhammad Aziz, Jeffrey S. Cross |
| Citation | Energies, Vol. 18, Issue 17, pp. 4568 |
| Pub. date | 2025, 8 |
| Creative Commons | The information is in the article. |



energies



Article

Selective Extraction and Hydrotreatment of Biocrude from Sewage Sludge: Toward High-Yield, Alkane-Rich, Low-Heteroatom Biofuels

Muhammad Usman, Shuo Cheng, Sasipa Boonyubol, Muhammad Aziz and Jeffrey S. Cross

Special Issue

New Trends in Biofuels and Bioenergy for Sustainable Development: 3rd Edition

Edited by




Prof. Dr. João Fernando Pereira Gomes and Dr. Toufik Boushaki



<https://doi.org/10.3390/en18174568>

Article

Selective Extraction and Hydrotreatment of Biocrude from Sewage Sludge: Toward High-Yield, Alkane-Rich, Low-Heteroatom Biofuels

Muhammad Usman ¹, Shuo Cheng ¹, Sasipa Boonyubol ¹, Muhammad Aziz ^{2,3,*} and Jeffrey S. Cross ^{1,*}

¹ Department of Transdisciplinary Science and Engineering, School of Environment and Society, Tokyo Institute of Technology, 2-12-1 Ookayama, Meguro-ku, Tokyo 152-8550, Japan; usman.m.aa@m.titech.ac.jp (M.U.)

² Institute of Industrial Science, The University of Tokyo, 4-6-1 Komaba, Meguro-ku, Tokyo 153-8505, Japan

³ Faculty of Mathematics and Science, Universitas Negeri Malang, Jl. Semarang 5, Malang 65145, Indonesia

* Correspondence: maziz@iis.u-tokyo.ac.jp (M.A.); cross.j.aa@m.titech.ac.jp (J.S.C.)

Abstract

This study investigates the hydrothermal liquefaction (HTL) of sewage sludge across a temperature range of 250–375 °C, combined with selective solvent extraction and catalytic hydrotreatment to produce high-quality biocrude. Four solvents including dichloromethane (DCM), hexane, ethyl butyrate (EB), and ethyl acetate (EA), were used to evaluate temperature-dependent extraction performance and product quality. Biocrude yields increased from 250 °C to a maximum at 350 °C for all solvents: hexane (9.3–18.1%), DCM (16.3–49.7%), EB (17.6–50.1%), and EA (9.6–23.5%). A yield decline was observed at 375 °C due to secondary cracking and gasification. Elemental analysis revealed that hexane and EB extracts had higher carbon (up to 61.6 wt%) and hydrogen contents, while DCM retained the most nitrogen (up to 3.96 wt%) due to its polarity. Sulfur remained below 0.5 wt% in all biocrudes. GC–MS analysis of 350 °C biocrudes showed fatty acids as dominant components (43–53%), especially palmitic acid, along with ketones, amides, and heterocyclic compounds. Hydrotreatment using Ni/SiO₂–Al₂O₃ significantly enhanced biocrude quality by increasing alkane content by 40–60% and reducing nitrogen levels by up to 75%, with higher heating values reaching 38–44 MJ/kg. These findings demonstrate the integrated potential of HTL process tuning, green solvent extraction, and catalytic upgrading for converting sewage sludge into cleaner, energy-dense biofuels.

Keywords: green solvents; hydrothermal liquefaction; sewage sludge; biocrude; waste-to-energy; sustainable resource management; energy recovery; hydrotreatment; biocrude upgrading; biofuel production; nitrogen reduction



Academic Editors: Fernando Rubiera González and Cristiano Varrone

Received: 26 July 2025

Revised: 15 August 2025

Accepted: 26 August 2025

Published: 28 August 2025

Citation: Usman, M.; Cheng, S.; Boonyubol, S.; Aziz, M.; Cross, J.S. Selective Extraction and

Hydrotreatment of Biocrude from Sewage Sludge: Toward High-Yield, Alkane-Rich, Low-Heteroatom Biofuels. *Energies* **2025**, *18*, 4568.

<https://doi.org/10.3390/en18174568>

Copyright: © 2025 by the authors. Licensee MDPI, Basel, Switzerland. This article is an open access article distributed under the terms and conditions of the Creative Commons Attribution (CC BY) license (<https://creativecommons.org/licenses/by/4.0/>).

1. Introduction

Sewage sludge (SS), the semi-solid byproduct of wastewater treatment plants (WWTPs), poses a rapidly escalating global environmental challenge. With the expansion of urban populations and industrial development, annual global SS production has surged, reaching estimates of 75–100 million dry tons [1]. Regions such as the European Union, the United States, China, and Japan collectively contribute tens of millions of tons annually [2–5]. The conventional disposal methods, including incineration, landfilling, and agricultural application, are increasingly constrained by environmental regulations, public health concerns, and rising operational costs [1,6–10]. These limitations under-

score an urgent need for sustainable sludge valorization strategies that not only mitigate environmental risks but also contribute to circular economy and energy recovery goals.

SS contains a substantial proportion of organics (30–80% depending on region) [11–14] and represents a valuable feedstock for liquid biofuels such as biodiesel and biocrude [15]. Its wide availability in urban areas offers dual benefits, supporting WWTP and reducing reliance on fossil fuels, while addressing transportation sector CO₂ emissions [15,16]. Previous approaches like lipid extraction and transesterification have shown potential but often require energy-intensive pretreatments, and leave residual sludge to manage [17–19]. Thermochemical routes such as pyrolysis can convert dried SS into bio-oil, biochar, and gases, yet the need for sludge drying, coupled with low-quality, oxygen- and nitrogen-rich oils, limits large-scale viability [20].

In recent years, hydrothermal liquefaction (HTL) has gained prominence as a viable thermochemical route for converting wet SS into biocrude, without the need for energy-intensive drying [21,22]. Operating under subcritical water conditions (typically 250–374 °C and 10–25 MPa), HTL can decompose complex organic matter into valuable products—primarily biocrude, along with aqueous phase organics, biochar, and gases [23–25]. Numerous studies have demonstrated the potential of HTL to yield significant amounts of energy-dense biocrude, making it a promising candidate for decentralized waste-to-fuel applications. However, key challenges remain, notably the high nitrogen (N) content (4.2% to 5.7%) and heteroatom-rich composition of SS-derived biocrude, which undermine its fuel quality, stability, and post-processing cost-effectiveness [26–28].

Efforts to enhance the quality of biocrude have primarily focused on optimizing HTL operating conditions or incorporating catalysts [26]. Parallel to this, solvent extraction plays a pivotal role in recovering biocrude from HTL mixtures. Traditional solvents such as dichloromethane (DCM) [29], acetone [30], methanol [8], and toluene [27] have been widely employed, but they are often associated with health hazards, environmental toxicity, and high volatility [26,28]. Moreover, polar solvents like DCM tend to extract a broad range of nitrogen-containing and oxygenated compounds, exacerbating the heteroatom burden in the biocrude [28]. In response to these drawbacks, recent literature has suggested exploring green solvents which are biodegradable, low-toxicity alternatives derived from renewable sources for bio-oil extraction [31]. Despite their growing relevance in fields such as pharmaceuticals and fine chemicals [31–33], their application in HTL biocrude extraction, particularly from protein-rich feedstocks like SS, remains largely unexplored.

To address this gap, a previous study by the authors of this paper [34] investigated the HTL of SS at a fixed temperature of 350 °C using conventional (DCM, hexane) and green solvents, ethyl acetate (EA) and ethyl butyrate (EB), for biocrude extraction. This study demonstrated that EB not only achieved the highest biocrude yield (50.1 wt%) but also significantly reduced nitrogen content (0.32 wt%), outperforming traditional solvents in both yield and quality. These findings established green solvent-assisted HTL as a promising pathway for low-nitrogen, high-energy biocrude production.

Building upon previous work [34], this study expands the scope by optimizing HTL across a broader temperature range (250–375 °C) and comparing the performance of conventional and green solvents under varying conditions. Additionally, the resulting HTL biocrudes were upgraded through hydrotreatment to evaluate their potential for biofuel applications and assess improvements in fuel quality. By providing extensive process-level insights and integrating both extraction and upgrading strategies, this study advances the field toward more practical and efficient biofuel production from SS.

2. Materials and Methods

2.1. Materials

Municipal dewatered SS used in this study was sourced from a wastewater treatment facility located in Tokyo, Japan. The plant employs the anaerobic–anoxic–aerobic (A2O) method for biological treatment and operates at a capacity of approximately 115,750 m³/day. A total of 1 kg of SS was collected and used consistently across all HTL experiments to maintain uniformity in feedstock composition and ensure comparability of results. The SS had an average moisture content of ~75%, making it ideal for direct HTL processing without the need for energy-intensive drying. Table 1 summarizes the key proximate and ultimate analysis of the dried SS, including elemental composition and higher heating value (HHV).

Table 1. Basic physical and fundamental elemental characteristics of the SS (Adapted from [35]).

| | | Proximate Analysis | | | | | |
|-----------------|-----------------|--------------------|------|------|------|----------------|----------------|
| SS Dewatered | Moisture | Volatiles | | | Ash | Fixed Carbon | |
| | (%) | wt% (dry basis) | | | | | |
| | 75 | 76 | | | 11.3 | 12.7 | |
| | | Ultimate Analysis | | | | | |
| SS Dewatered | Ash | C | H | N | S | O ^a | HHV (MJ/kg) |
| | wt% (dry basis) | | | | | | |
| | 11.3 | 44.34 | 6.37 | 5.89 | 0.62 | 31.48 | 18.52 |

^a—oxygen composition calculation equation. ^a O% = 100% – C% – H% – N% – S%.

For biocrude extraction, four high-purity solvents were used. Dichloromethane (DCM) and hexane are widely reported in previous studies and served as reference conventional solvents. In contrast, ethyl acetate (EA) and ethyl butyrate (EB), derived from renewable resources and known for their low toxicity and biodegradability, were selected as green solvent alternatives. All solvents were of analytical grade and procured from Sigma-Aldrich (St. Louis, MO, USA).

To upgrade the crude biocrude, a commercially available Ni/SiO₂–Al₂O₃ catalyst containing approximately 65 wt% nickel was utilized without any pretreatment. This catalyst was chosen for its cost-effectiveness, non-noble metal composition, and proven performance in hydrodeoxygenation (HDO) applications. Compared to conventional sulfided catalysts (e.g., CoMo/Al₂O₃, NiMo/Al₂O₃) or noble metals (Pt, Pd, Ru), the selected Ni-based catalyst offers a practical alternative [36,37], eliminating the need for pre-sulfidation while demonstrating efficacy in upgrading pyrolysis oils, vegetable oils, and HTL-derived biocrudes [21,28,38].

2.2. HTL Experiments

The experimental methodology for HTL was adapted from a previous study [34], in which the process was conducted at a fixed temperature of 350 °C. In the present work, the same reactor setup and procedural framework were employed, with key modifications introduced to evaluate temperature-based process optimization.

All experiments were performed using 20 mL mini-autoclave batch reactors composed of 1/2-inch 316 stainless steel components, sealed with in-house fabricated expanded graphite gaskets to ensure durability under high-temperature conditions. The sludge-to-water loading ratios varied between 1:9 and 2:8 (*w/w*), and the HTL experiments were

conducted across a temperature range of 250–375 °C, with a fixed residence time of 1 h. Temperature was increased at a controlled rate of ~10 °C/min, and each reaction was repeated in duplicate with 10 trials in total to ensure reproducibility. The HTL temperature range of 250–375 °C was selected to comprehensively evaluate the effect of reaction severity on the SS feedstock, with the aim of assessing overall conversion efficiency and optimizing solvent extraction performance. This range covers conditions commonly used for wet biomass HTL and enables identification of the most favorable operating conditions for biocrude production.

Following the reaction, reactors were rapidly quenched in a water bath. The reaction mixture was extracted with 20 mL of DCM, hexane, EA, or EB under magnetic stirring for 30 min. The extraction duration of 30 min was optimized and chosen based on previously reported protocols [34], which demonstrated it as sufficient for maximum biocrude recovery, ensuring consistent and efficient extraction across all solvent tests. Solids were separated via filtration (through a 110 mm filter paper (Japanese Industrial Standard (JIS) P 3801 Class 1 with a thickness of 0.20 mm)) and dried at 105 °C for 24 h. The aqueous and organic (biocrude) phases were separated using a separating funnel. Solvents were recovered using rotary evaporation (for DCM, hexane, and EA) or Soxhlet extraction (for EB due to its higher boiling point), with a recovery rate of ~90–95%.

To avoid redundancy, the detailed experimental setup, mass balance calculations, and product yield formulas can be referred to in an earlier publication [34]. Only the experimental workflow is presented here for clarity (see Figure 1).

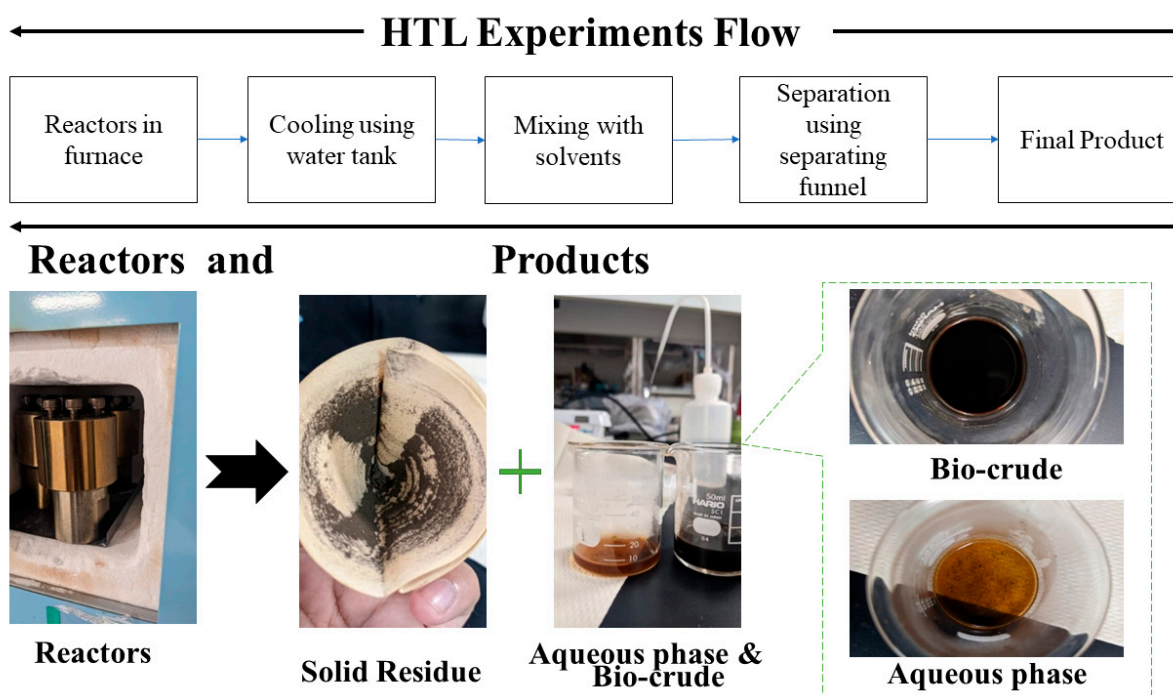


Figure 1. HTL of SS experimental flow and products separation.

2.3. Hydrotreatment (Hydrogenation Upgrading) of HTL Biocrude

The hydrotreatment (HDT) experiments were conducted using a 100 mL high-pressure portable reactor (TVS-1, Taiatsu Techno Corp., Tokyo, Japan), as detailed in Figure S1 in the Supplementary Materials, which provides specifications of the reactor design. Equipped with thermocouples, the reactor allowed for precise temperature monitoring both inside and outside, as well as within the heating jacket. A dedicated temperature controller (TS-K, AS One Corp., Osaka, Japan) was utilized to regulate and monitor the temperature throughout the process.

Each HDT experiment maintained a biocrude-to-catalyst mass ratio of 20:1, with the catalyst loading and hydrogen pressure (5 MPa) adopted directly from recent hydrotreatment studies on HTL biocrudes [28], where these parameters were shown to provide high conversion efficiency and effective catalyst utilization under batch operation. Specifically, 0.5 g of catalyst and 10 g of HTL biocrude were loaded into the reactor. The reactor then underwent three purges with 0.8 MPa of nitrogen, followed by a 10 min vacuuming process using a vacuum pump (G-10DA, ULVAC Inc., Miyazaki, Japan) with a pumping speed of 10–12 L/min to remove residual air and nitrogen. Finally, the reactor was charged with 5 MPa of hydrogen for 5 min to ensure uniform hydrogen pressure.

The hydrotreatment temperature range of 180–220 °C was determined by the maximum safe operating limit of the reactor (230–250 °C) and the need to remain within an effective upgrading window such as operational optimization and economic feasibility. Hydrogenation processes typically require high temperatures and pressures, which incur significant costs and operational challenges [39].

The reactor temperature was gradually increased from room temperature to 180, 200, and 220 °C at a consistent heating rate of approximately 10 °C/min. Subsequently, the reactor was maintained at the desired temperature for 60 min. After each experiment, the heating jacket was disassembled, and the reactor was rapidly cooled using a water tank to halt any residual reactions. Depressurization in a fume hood safely expelled any remaining gases, after which the liquid and solid products were extracted from the reactor. The liquid product was then filtered through a 90 mm filter paper (JIS P 3801 Class 1 with a thickness of 0.20 mm), and the liquid yield was calculated using Equation (1). All experiments were conducted in duplicate and repeated 10 times for accuracy and reproducibility.

$$\text{HDT Liquid yield (\%)} = \frac{\text{weight of liquid product}}{\text{weight of biocrude}} \times 100\% \quad (1)$$

2.4. Product Analysis or Characterization

The analytical procedures used for characterizing HTL biocrude in this study were consistent with those detailed in previous work [34]. Briefly, elemental analysis (CHNS), higher heating value (HHV) estimation via the Dulong equation were carried out as previously described. Gas chromatography–mass spectrometry (GC–MS) analysis was also performed using the same instrumentation and protocols to identify and categorize chemical compounds in the biocrude.

In the present study, these established characterization methods were extended to evaluate not only the HTL biocrudes extracted with various solvents but also the hydrotreatment (HDT)-derived liquid products. The GC–MS analysis was used to assess compositional shifts post-upgrading, while elemental analysis quantified reductions in nitrogen and heteroatom content. This enabled a comparative assessment of solvent impact and HDT effectiveness in improving the biocrude's suitability for biofuel applications.

3. Results

3.1. HTL Product Yields

The results presented in Figure 2 illustrate the product yields obtained from HTL of SS at various temperatures while maintaining a consistent 1:9 sludge-to-water ratio. The total mass of the collected products accounted for nearly 100% of the dry basis SS feedstock, with a potential margin of loss ($\pm 5\%$) considered due to factors such as volatile compound evaporation during solvent removal, water formation, and experimental errors.

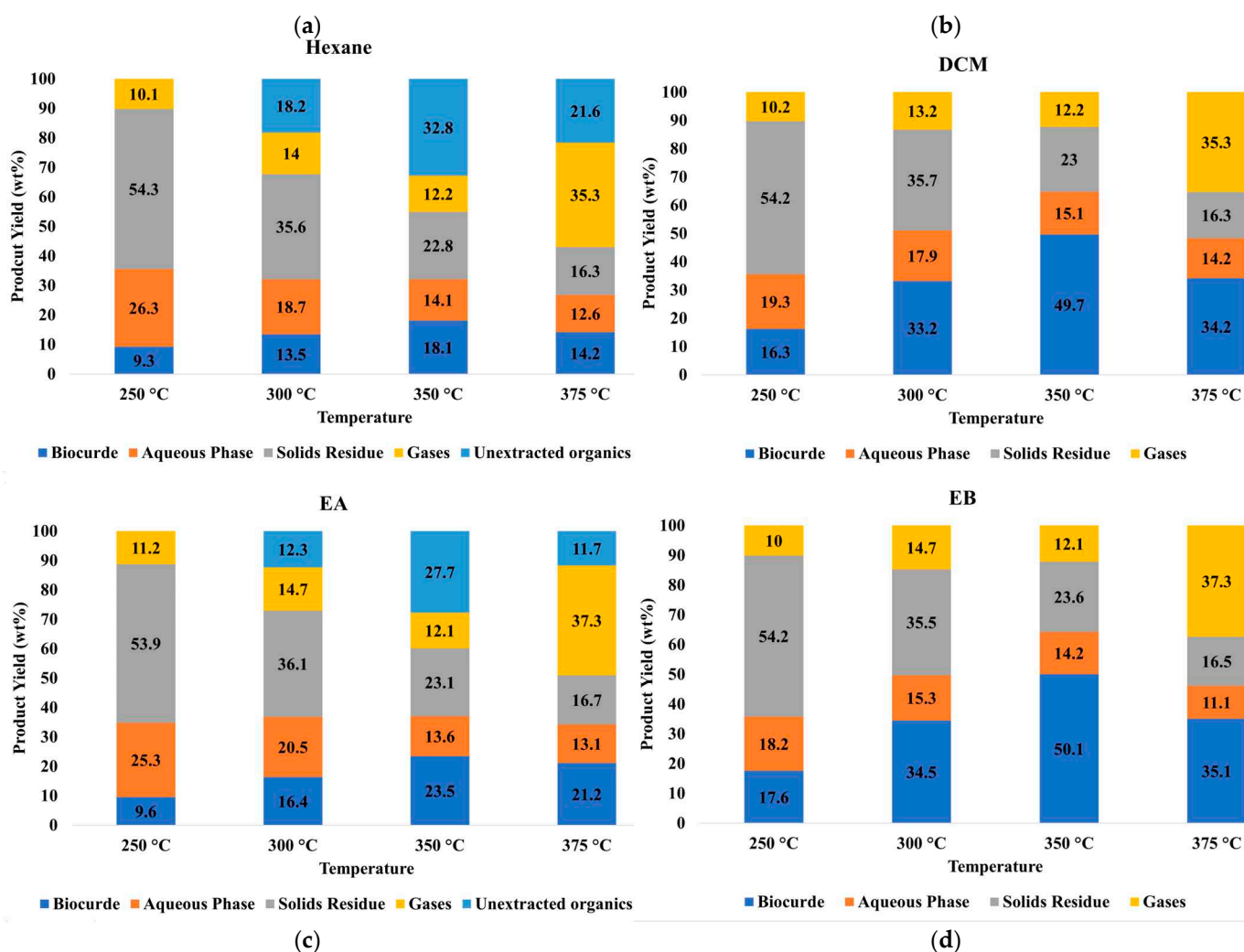


Figure 2. HTL product yields using a 1:9 sludge-to-water ratio at different temperatures using (a) Hexane, (b) DCM, (c) EA and (d) EB.

Analysis of the biocrude yield revealed an initial increase from 250 to 350 °C, followed by a decrease at 375 °C. Remarkably, the highest biocrude yield was achieved at 350 °C, showcasing the effectiveness of all four extraction solvents, DCM (49.7 wt%), hexane (18.1 wt%), EB (50.1 wt%), and EA (23.5 wt%) in the process. These fluctuations in biocrude extraction yields underscore the distinctive solvating capabilities of each solvent and their influence on extraction efficiency.

Furthermore, a significant decline in biocrude yields was observed at 375 °C for all four extraction solvents. Specifically, a reduction of 31.11% was noted with DCM, 21.15% with hexane, 29.94% with EB, and 9.78% with EA, highlighting the impact of temperature on biocrude production efficiency across different solvent systems.

At 250 °C, a relatively low temperature, hydrolysis reactions are predominant in SS HTL. Hydrolysis involves breaking chemical bonds with the addition of water molecules, converting complex organic molecules into simpler, more reactive compounds. However, due to the mild temperature, hydrolysis occurs at a slower rate, resulting in a modest biocrude yield.

As the temperature increases to 300 °C, hydrolysis reactions escalate significantly, and cracking reactions become more prominent due to increased thermal energy. Higher temperatures provide the molecules with more kinetic energy, allowing them to overcome the activation energy barrier required for cleavage. This results in the fragmentation of larger,

more complex organic compounds into smaller, more volatile constituents. Essentially, thermal energy facilitates the breaking of chemical bonds, leading to cracking reactions and an increase in biocrude yield. Cracking reactions, starting at 300 °C or above, contribute to the breakdown of complex organic compounds in the SS, generating a greater abundance of volatile hydrocarbons and other organic compounds [40,41].

The temperature of 350 °C represents an optimal condition for SS HTL, where the balance between hydrolysis and cracking reactions is finely tuned. The elevated temperature accelerates both reactions, allowing for efficient decomposition of organic matter. Hydrolysis continues to play a key role in breaking down complex molecules, while cracking further contributes to the release of valuable biocrude constituents. This temperature range strikes an ideal equilibrium, resulting in the highest biocrude yield.

Beyond the optimal range, thermal cracking reactions become increasingly dominant. The higher temperature accelerates the rate of cracking reactions, leading to the decomposition of biocrude compounds into smaller, less valuable molecules. Additionally, secondary reactions, such as polymerization, may occur, forming larger, less volatile compounds. These reactions reduce the overall yield of the desired biocrude, explaining the observed decline at 375 °C.

Consistent findings across diverse feedstock varieties underscore a compelling empirical trend: within the temperature range of 280 to 350 °C, the biocrude yield demonstrates a pronounced, positive correlation. However, as the temperature extends beyond this critical range, a notable inverse relationship emerges, leading to a discernible reduction in biocrude yield [42–46].

The decrease in both aqueous phase and solid residue yields between 250 and 375 °C can be attributed to the intensification of thermal decomposition, increased volatility of organic components, and the efficient conversion of organic solids into valuable products like biocrude. At higher temperatures, organic solids are more readily converted into gases and biocrude, leaving less material in the form of solid residue and aqueous phase [43,46,47]. Additionally, there is a noteworthy increase in gas yields at elevated temperatures, attributed to thermal decomposition, volatilization, and cracking reactions. These observed trends underscore the complex and temperature-dependent nature of SS HTL, where diverse reactions influence the distribution of product fractions [48]. It is important to note that n-hexane, a non-polar solvent, and EA, a moderately polar aprotic solvent, exhibited lower biocrude yields compared to EB and DCM. Literature-reported solvent polarity indices (PI) and Hansen solubility parameters (HSP) confirm that EA and EB are moderately polar but may be considered relatively non-polar in certain contexts, as they contain substantial non-polar alkyl groups in addition to polar carbonyl (C=O) and ether oxygen functionalities (Table 2). DCM is classified as polar, while n-hexane is non-polar. The comparatively lower PI/HSP values of n-hexane and EA relative to DCM, along with differences in solvation selectivity, likely limited their extraction of certain polar and oxygenated compounds from the biocrude. This limitation appeared to leave a greater fraction of organics associated with the solid phase during separation, leading to their calculation as unextracted organics. Similar lower extraction efficiencies for non-polar solvents such as hexane have also been reported in previous HTL studies [28,34]. Similar results, with $\pm 5\%$ variations, were observed for the 2:8 sludge-to-water ratio, as detailed in Table S1 in the Supplementary Materials.

Table 2. Polarity indices (PI) and Hansen solubility parameters (HSP) of solvents used in this study.

| Solvent | Polarity Index | Hansen Solubility Parameters (MPa ^{0.5}) | Boiling Point (°C) | Density (g/mL) | Reference |
|---------|----------------|--|--------------------|----------------|-----------|
| Hexane | ~0.1–0.2 | δD: 14.9, δP: 0, δH: 0 | 68.7 | 0.654 | [49,50] |
| DCM | 3.1 | δD: 17.0, δP: 7.3, δH: 7.1 | 39.8 | 1.33 | [51,52] |
| EA | 4.4 | δD: 15.8, δP: 5.3, δH: 7.2 | 77 | 0.902 | [52,53] |
| EB | 3.1–3.7 | δD: 16.1, δP: 3.7, δH: 5.0–6.4 | 121 | 0.879 | [52,54] |

“δD = dispersion forces, δP = polar forces, δH = hydrogen bonding”.

3.2. Characterization of HTL Biocrude

Table 3 shows the elemental composition and HHV of biocrude products obtained from HTL of SS were analyzed to assess their quality across various temperatures (250–375 °C) and extraction solvents (DCM, hexane, EB, and EA). These parameters are key indicators of the energy potential and fuel suitability of HTL-derived biocrude.

Carbon and hydrogen contents, which are directly correlated with the energy content of bio-oil, increased with temperature up to 350 °C for all solvents. This behavior is attributed to enhanced thermal decomposition and conversion of organic components into hydrocarbon-rich compounds at elevated temperatures. The highest carbon contents were observed at 350 °C for biocrudes extracted with hexane (61.62 wt%) and EB (58.87 wt%), indicating that these non-polar solvents are more effective in selectively extracting hydrocarbon fractions. Similarly, the hydrogen content peaked at 12.3 wt% with hexane at 350 °C, further confirming the efficiency of non-polar solvents in isolating hydrogen-rich, aliphatic compounds.

However, a reduction in both carbon and hydrogen contents was noted at 375 °C across all solvents. This decline is likely due to excessive cracking reactions and gas formation at higher temperatures, which degrade larger hydrocarbon molecules and reduce the overall energy density of the remaining biocrude. For instance, carbon content in DCM-derived biocrude dropped from 54.9 wt% at 350 °C to 37.78 wt% at 375 °C, and its HHV decreased from 22.44 to 15.44 MJ/kg, highlighting the thermal instability of biocrude compounds beyond optimal processing conditions.

Nitrogen content in the biocrude varied significantly with solvent polarity and temperature. DCM-extracted biocrudes consistently exhibited higher nitrogen levels (1.3–3.96 wt%), due to the solvent’s moderate polarity and its ability to solubilize polar nitrogen-containing compounds formed from protein degradation in the sludge. These compounds, including amines, amides, and heterocycles, are known to reduce fuel stability and increase NO_x emissions upon combustion. In contrast, non-polar solvents such as hexane and EA extracted biocrudes with nitrogen levels as low as 0.12–0.23 wt%, minimizing the presence of nitrogenous impurities. The data suggests that solvent selection plays a critical role in managing nitrogen content in HTL biocrude, which is a key consideration for downstream upgrading and emissions control.

Sulfur content, though generally low, followed similar solvent-dependent patterns. DCM and EB extracted detectable sulfur in the range of 0.20–0.53 wt%, with peak values at 350 °C. In contrast, sulfur was undetectable (below analytical limits) in biocrudes extracted with hexane and EA at all temperatures, indicating these solvents are less prone to co-extracting sulfur-containing compounds. This distinction is important for refining compatibility, as sulfur contributes to catalyst poisoning and requires expensive desulfurization steps during fuel processing.

Table 3. Elemental compositions of extracted biocrude from SS HTL using different solvents.

| Solvents | Temperature (°C) | Biocrude Yields | C | H | N | S | O ^a | HHV MJ/kg |
|----------|------------------|-----------------|----------------------|-------------|-------------|-------------|----------------|--------------|
| | | | wt.% on Dry SS Basis | | | | | |
| DCM | 250 | 16.3 ± 0.82 | 18.01 ± 0.9 | 2.26 ± 0.11 | 1.3 ± 0.06 | 0.20 ± 0.01 | 11.03 ± 0.55 | 7.36 ± 0.37 |
| | 300 | 33.2 ± 1.66 | 36.67 ± 1.83 | 4.61 ± 0.23 | 2.65 ± 0.13 | 0.39 ± 0.02 | 22.46 ± 1.12 | 14.99 ± 0.75 |
| | 350 | 49.7 ± 2.49 | 54.9 ± 2.74 | 6.9 ± 0.34 | 3.96 ± 0.2 | 0.53 ± 0.03 | 33.62 ± 1.68 | 22.44 ± 1.12 |
| | 375 | 34.2 ± 1.71 | 37.78 ± 1.89 | 4.75 ± 0.24 | 2.72 ± 0.14 | 0.35 ± 0.02 | 23.13 ± 1.16 | 15.44 ± 0.77 |
| Hexane | 250 | 9.3 ± 0.47 | 31.66 ± 1.58 | 6.32 ± 0.32 | 0.12 ± 0.11 | NA | 13.28 ± 0.66 | 17.39 ± 0.87 |
| | 300 | 13.5 ± 0.68 | 45.96 ± 2.3 | 9.17 ± 0.46 | 0.17 ± 0.01 | NA | 19.28 ± 0.96 | 25.24 ± 1.26 |
| | 350 | 18.1 ± 0.91 | 61.62 ± 3.08 | 12.3 ± 0.62 | 0.23 ± 0.01 | NA | 25.85 ± 1.29 | 33.84 ± 1.69 |
| | 375 | 14.2 ± 0.71 | 48.34 ± 2.42 | 9.65 ± 0.48 | 0.18 ± 0.01 | NA | 20.28 ± 1.01 | 26.55 ± 1.33 |
| EB | 250 | 17.6 ± 0.88 | 20.68 ± 1.03 | 3.22 ± 0.16 | 0.11 ± 0.01 | NA | 11.1 ± 0.56 | 9.62 ± 0.48 |
| | 300 | 34.5 ± 1.72 | 40.54 ± 2.03 | 6.32 ± 0.32 | 0.22 ± 0.01 | NA | 21.76 ± 1.09 | 18.85 ± 0.94 |
| | 350 | 50.1 ± 2.51 | 58.87 ± 2.94 | 9.18 ± 0.46 | 0.32 ± 0.02 | 0.03 ± 0.00 | 31.6 ± 1.58 | 27.38 ± 1.37 |
| | 375 | 35.1 ± 1.76 | 41.24 ± 2.06 | 6.43 ± 0.32 | 0.22 ± 0.01 | 0.02 ± 0.00 | 22.14 ± 1.11 | 19.18 ± 0.96 |
| EA | 250 | 9.6 ± 0.48 | 19.33 ± 0.97 | 3.46 ± 0.17 | 0.09 ± 0.0 | NA | 17.96 ± 0.9 | 8.26 ± 0.41 |
| | 300 | 16.4 ± 0.82 | 33.02 ± 1.65 | 5.91 ± 0.3 | 0.16 ± 0.01 | NA | 30.68 ± 1.53 | 14.12 ± 0.71 |
| | 350 | 23.5 ± 1.18 | 47.31 ± 2.37 | 8.47 ± 0.42 | 0.23 ± 0.01 | NA | 43.96 ± 2.2 | 20.23 ± 1.01 |
| | 375 | 21.2 ± 1.06 | 42.68 ± 2.13 | 7.64 ± 0.38 | 0.21 ± 0.01 | NA | 39.66 ± 1.98 | 18.25 ± 0.91 |

^a—O% = 100% – C% – H% – N% – S%. NA: Below detection limit.

Oxygen content, calculated by difference, decreased with rising temperature up to 350 °C, reflecting progressive deoxygenation and the removal of polar functional groups such as hydroxyl, carbonyl, and carboxyl. DCM-extracted biocrude at 250 °C contained 11.03 wt% oxygen, which increased to 33.62 wt% at 350 °C due to concurrent accumulation of nitrogenous and oxygenated organics. However, the lowest oxygen levels were observed in biocrudes extracted with hexane and EB, particularly at 350 °C (25.85 wt% and 31.6 wt%, respectively), confirming their selectivity for less polar, deoxygenated compounds.

HHV is a critical measure of energy recovery potential. Among all samples, hexane-extracted biocrude at 350 °C achieved the highest HHV of 33.84 MJ/kg, aligning with its high carbon and hydrogen content and low heteroatom presence. EB also produced a high-quality biocrude with an HHV of 27.38 MJ/kg at the same temperature. DCM and EA yielded lower HHVs due to higher nitrogen and oxygen contents, although a general upward trend in HHV was evident from 250 to 350 °C for all solvents. At 375 °C, a noticeable reduction in HHV occurred, indicating that over-cracking not only reduces yield but also degrades fuel quality.

In summary, the temperature of 350 °C consistently produced biocrudes with optimal elemental profiles and highest energy content, especially when extracted with non-polar solvents. The results confirm that both process temperature and solvent polarity significantly influence biocrude composition. Non-polar solvents such as hexane and EB are more effective in isolating high-energy, hydrocarbon-rich compounds with minimal heteroatoms, making them suitable for producing cleaner biocrudes with improved fuel properties. These insights are essential for developing integrated HTL processes and post-treatment strategies aimed at sustainable biofuel production from municipal SS.

Considering the biocrude yield results obtained at 350 °C, this temperature was selected for further investigation due to its potential for maximizing biocrude recovery from SS HTL.

Chemical Compounds Composition in Biocrudes

The composition of volatile compounds in the HTL-derived biocrudes at 350 °C was evaluated using GC-MS. The corresponding total ion chromatograms (TIC) and compound identification tables, including retention times and peak areas, are presented in the Supplementary Material (Figures S2–S5 and Tables S2–S5). For clarity and comparison, the compounds were categorized into ten major classes based on their chemical functionalities and relevance to biofuel applications: fatty acids, heterocyclic aromatics, ketones, esters, lipids, fatty amides, alcohols, phenolic compounds, terpenoids, and alkanes (Figure 3).

Among these, fatty acids were consistently dominant across all extraction solvents, representing over 40% of the total peak area. Hexane-extracted biocrude exhibited the highest relative abundance of fatty acids (52.95%), followed by EA (48.75%), DCM (43.92%), and EB (43.44%). The widespread presence of *n*-hexadecanoic acid (palmitic acid), ranging between 20 and 22% peak area, is indicative of lipid hydrolysis, a common reaction pathway in HTL of sludge rich in triglycerides. This trend is further supported by reports that SS from Tokyo contains a substantial organic fraction of up to approximately 60% to 80% of its dry matter, of which lipids constitute around 30% to 35% [55,56]. Such a high lipid content explains the prevalence of fatty acid derivatives in the resulting biocrude, highlighting their critical contribution to the energy-rich hydrocarbon pool produced during HTL.

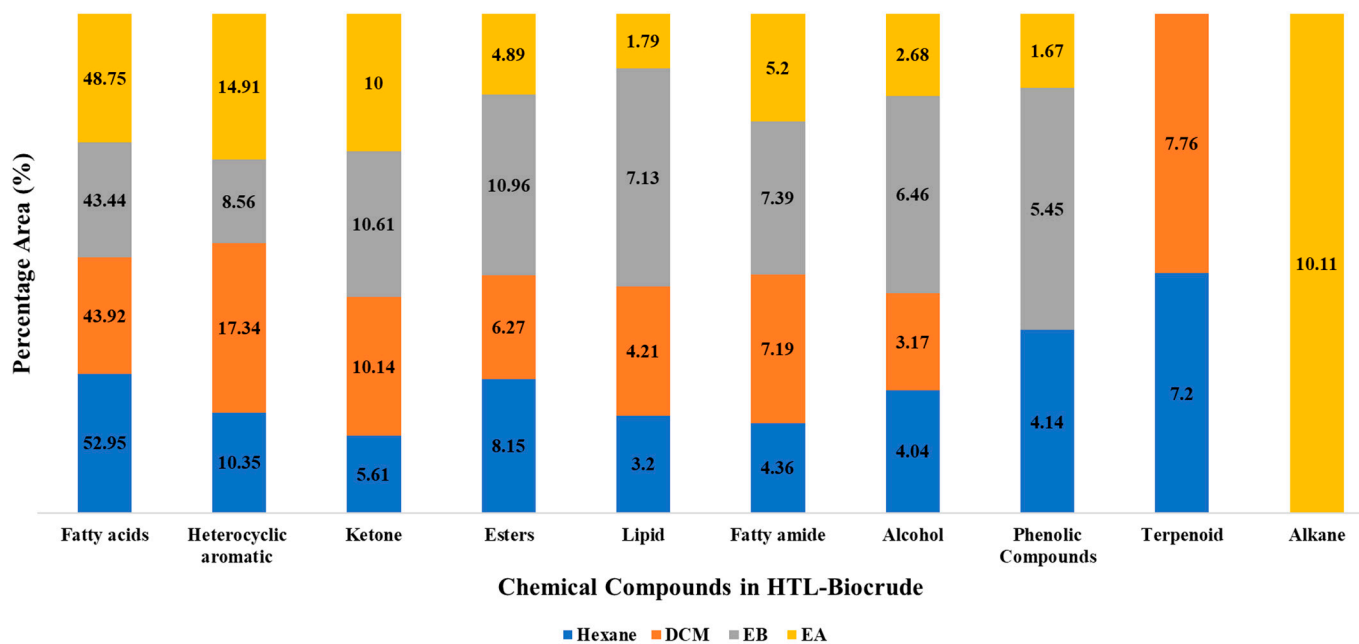


Figure 3. Chemical composition of the HTL biocrude extracted with different solvents.

Heterocyclic aromatics, including N- and O-containing rings such as substituted pyrazines and benzene derivatives, were the second most prominent class. DCM-extracted biocrude exhibited the highest levels (17.05%), reflecting its stronger solvating ability for polar and moderately polar compounds. In contrast, EB and hexane extracted lower quantities of these compounds, which can be linked to their limited affinity for polar heterocycles. These compounds largely originate from the degradation and rearrangement of proteinaceous matter in SS, potentially enhanced by Maillard-type reactions under HTL conditions [40,57–59].

Ketones were also identified in all extracts, most notably 2-cyclopenten-1-one derivatives. These compounds are typically formed from carbohydrate decomposition and subsequent cyclization [60]. Their presence in comparable proportions across solvents (7–11%) suggests a common origin, although extraction efficiency may differ slightly due to solvent polarity.

Esters and lipids appeared more frequently in EB-extracted biocrude, indicating EB's enhanced solubility for medium-polarity and lipid-derived compounds. The relative abundance of fatty amides such as hexadecanamide and octadecanamide is closely associated with protein degradation pathways and subsequent amide-forming reactions during HTL. These nitrogen-containing species were more prominent in DCM and EB extracts, reflecting their intermediate polarity and capacity to extract bio-nitrogen compounds.

Alcohols and phenolic compounds were moderately abundant in EB and hexane extracts. Phenols such as phenol and p-cresol are generally derived from lignin or protein breakdown [61], and their detection supports the complex organic makeup of SS. The absence of phenols in DCM-extracted biocrude may suggest limited solubility or potential suppression during extraction.

Notably, terpenoids, identified in both hexane and DCM extracts, reflect the plant-derived fraction or microbial biosynthetic origin of the feedstock [62–64]. These compounds have desirable fuel characteristics and indicate the biochemical complexity of municipal sludge. Alkanes, primarily detected in EA extracts, suggest selective recovery of non-polar hydrocarbons, likely aided by EA's moderate polarity and compatibility with aliphatic species.

Overall, the GC–MS profile reveals how solvent selection significantly influences the chemical fingerprint of HTL biocrudes. The classification scheme applied in this study (see Supplementary Tables S2–S5) provides a structured overview of compound types, emphasizing the importance of extraction polarity in determining the fuel-quality precursors and contaminant profiles in the product stream.

3.3. Hydrotreated Liquid Product Yield and Elemental Analysis

Figure 4 illustrates the liquid yield of organics obtained from the hydrotreatment (HDT) of HTL biocrude extracted using four different solvents within a temperature range of 180 to 220 °C.

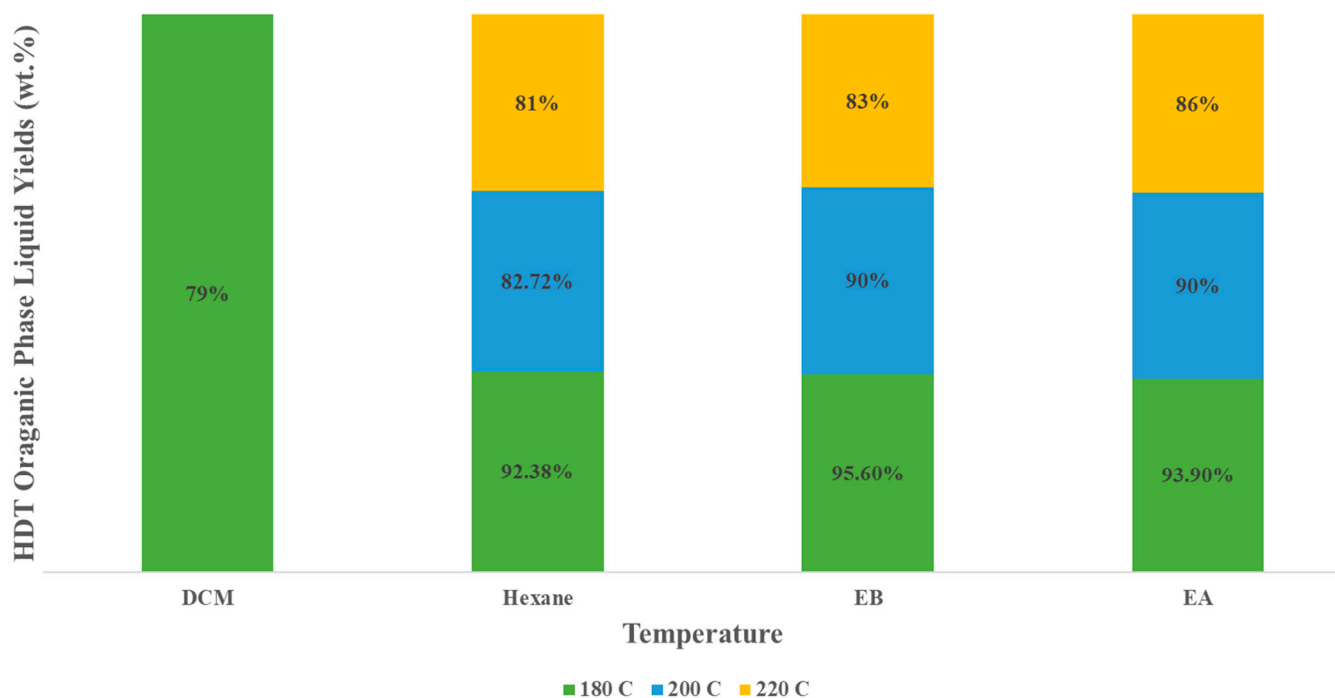


Figure 4. The organic phase liquid yields at different temperatures for all solvent-extracted biocrude.

At 180 °C, the highest organic phase liquid yield was achieved, with values of 79 wt%, 91.3 wt%, 92.6 wt%, and 92.1 wt% for DCM, hexane, EB, and EA, respectively. However, as the temperature increased from 180 °C to 220 °C, this yield gradually decreased, with reductions of 11.92% for hexane, 8.34% for EB, and 6.57% for EA at 220 °C. Notably, the aqueous phase yield increased with rising temperature as shown in Table 4, possibly due to the removal of oxygen in the form of water during the upgrading process.

DCM-extracted biocrude exhibited distinct behavior during HDT, with an initial 79% organic phase at 180 °C, followed by solidification. This phenomenon is noticed due to the formation of acids during the HDT process, as reported in previous studies [65,66]. Interestingly, recent investigations uncovered elevated chloride levels in DCM-extracted biocrude, possibly resulting from interactions between DCM and biocrude molecules [28], though chloride content analysis was not performed in this study to further explore this aspect.

Analysis of the elemental compositions of the HDT liquid organic phase as presented in Table 4 revealed an increase in quality from 180 to 220 °C in terms of C, H, N, S, and O contents for hexane, EB, and EA.

Table 4. The hydrotreated liquid products and elemental composition.

| HDT of HTL Biocrude | DCM | | | Hexane | | | EB | | | EA | | |
|----------------------------|------------------------------|-----|-----|----------------|----------------|----------------|----------------|----------------|----------------|----------------|----------------|----------------|
| | 180 | 200 | 220 | 180 | 200 | 220 | 180 | 200 | 220 | 180 | 200 | 220 |
| Temperature (°C) | | | | | | | | | | | | |
| Organic liquid yield (wt%) | 79 ± 0.35 | 0 | 0 | 90.38 ± 0.27 | 80.02 ± 0.17 | 79.6 ± 0.15 | 93.5 ± 0.07 | 90.2 ± 0.10 | 85.7 ± 0.10 | 91.2 ± 0.05 | 88.6 ± 0.10 | 85.2 ± 0.10 |
| Aqueous phase (wt%) | 0 | 0 | 0 | 2.0 ± 0.05 | 2.7 ± 0.05 | 3.1 ± 0.05 | 2.1 ± 0.05 | 2.9 ± 0.05 | 3.3 ± 0.05 | 2.3 ± 0.05 | 2.7 ± 0.05 | 3 ± 0.05 |
| | Elemental Compositions (wt%) | | | | | | | | | | | |
| C | 56.1 ± 0.10 | - | - | 68.7 ± 0.10 | 70.87 ± 0.10 | 74.33 ± 0.10 | 65.3 ± 0.10 | 69.8 ± 0.10 | 72.18 ± 0.10 | 54.8 ± 0.10 | 57.75 ± 0.05 | 60.35 ± 0.05 |
| H | 7.3 ± 0.10 | - | - | 11.79 ± 0.05 | 13.92 ± 0.05 | 14.71 ± 0.10 | 10.94 ± 0.05 | 12.5 ± 0.05 | 13.91 ± 0.05 | 9.71 ± 0.01 | 10.2 ± 0.05 | 11.81 ± 0.05 |
| N | 3.93 ± 0.01 | - | - | 0.20 ± 0.01 | 0.17 ± 0.01 | 0.15 ± 0.01 | 0.28 ± 0.01 | 0.23 ± 0.01 | 0.21 ± 0.01 | 0.20 ± 0.01 | 0.19 ± 0.01 | 0.19 ± 0.01 |
| S | 0.50 ± 0.01 | - | - | NA | NA | NA | NA | NA | NA | NA | NA | NA |
| O ^a | 32.17 ± 0.101 | - | - | 19.31 ± 0.05 | 15.04 ± 0.10 | 10.81 ± 0.05 | 23.48 ± 0.08 | 17.47 ± 0.05 | 13.7 ± 0.05 | 35.29 ± 0.08 | 31.86 ± 0.05 | 27.65 ± 0.05 |
| H/C (molar ratio) | 1.56 ± 0.01 | | | 2.05 ± 0.01 | 2.35 ± 0.01 | 2.37 ± 0.01 | 2.01 ± 0.05 | 2.14 ± 0.02 | 2.31 ± 0.01 | 2.12 ± 0.01 | 2.11 ± 0.01 | 2.34 ± 0.01 |
| N/C (molar ratio) | 0.06 ± 0.00 | | | 0.002 ± 0.0001 | 0.002 ± 0.0001 | 0.001 ± 0.0001 | 0.002 ± 0.0001 | 0.002 ± 0.0001 | 0.002 ± 0.0001 | 0.003 ± 0.0005 | 0.002 ± 0.0000 | 0.002 ± 0.0000 |
| HHV (MJ/kg) | 23.68 ± 0.03 | | | 36.66 ± 0.10 | 41.24 ± 0.05 | 44.31 ± 0.05 | 33.54 ± 0.05 | 38.39 ± 0.05 | 41.91 ± 0.05 | 26.1 ± 0.05 | 28.42 ± 0.05 | 32.38 ± 0.10 |

^a—O% = 100% − C% − H% − N% − S%, NA: Below detection limit.

This improvement is primarily attributed to the removal of heteroatoms such as N, S, and O. The N content exhibited a consistent decrease with increasing HDT temperature, with the most substantial decreases recorded in hexane-extracted biocrude at approximately 34.78% at 220 °C. EB and EA extracted from HTL biocrude also experienced notable reductions in N content, reaching roughly 34.37% and 17.39%, respectively. This reduction in N content during HDT can be attributed to the breakdown and removal of N-containing compounds derived from proteins and amino acids in the biomass feedstock. As the temperature increases in the HDT process, these N-rich molecules are chemically transformed and rendered more volatile, facilitating their removal [67]. As the temperature increases in the HDT process, these nitrogen-rich molecules are chemically transformed and rendered more volatile, facilitating their removal.

The absence of detectable S contents in the HTL biocrude extracted by hexane, EB, and EA following the HDT process can be attributed to the effective removal of sulfur-containing compounds during the HDT. However, it is noteworthy that the S contents in the HTL biocrude prior to the HDT were already negligible, as indicated in Table 3. The choice of extraction solvents employed in this study may have contributed to the exceptionally low sulfur content in the HTL biocrude. Moreover, the subsequent HDT process likely played a significant role in eliminating any residual sulfur-containing compounds through hydrodesulfurization [67,68], ultimately yielding an organic liquid phase with undetectable sulfur levels.

The O content in the organic liquid yield obtained through HDT exhibited a notable decrease with increasing temperature. The most significant reductions were observed at 220 °C, where the oxygen content decreased by 58.18% for hexane-extracted biocrude, 56.64% for EB-extracted biocrude, and 37.10% for EA-extracted biocrude compared to their respective HTL biocrudes (Table 2). The smaller relative decrease in O% for EA-derived hydrogenated oil can be attributed to the compositional characteristics of the EA-extracted biocrude. Due to its polarity, EA extracts higher amounts of oxygen-containing compounds (e.g., fatty acids and heterocyclic compounds (see Figure 3)), which are more resistant to complete deoxygenation under the mild hydrotreatment conditions applied (180–220 °C, 5 MPa H₂) (see Figure 5). In contrast, EB and n-hexane extracts contain fewer of these refractory oxygenated species, allowing for a greater relative reduction in oxygen content under the same conditions.

The reduction in O content during HDT can be attributed to several chemical transformations occurring at elevated temperatures. One potential pathway involves the removal of hydroxy groups (OH) as water (H₂O) through hydrogenolysis reaction mechanisms, which include dehydration and hydrogenation reactions [68]. Additionally, the increased oxygen removal could also be linked to the formation of an aqueous phase during HDT in this study, contributing to the decreased oxygen content in the organic liquid yield. Hydrogenolysis reactions, particularly the removal of hydroxy groups as water, tend to occur effectively in the presence of a catalyst and under atmospheric pressure, usually at temperatures ranging between 150 and 200 °C as reported [69]. This process is facilitated by the increased temperature during HDT, leading to the removal of O-rich functional groups from the biocrude and the formation of more stable, less oxygenated compounds.

On the other hand, the elemental compositions in the HDT liquid yield of DCM-extracted biocrude remained consistent with those reported in the HTL biocrude due to the initially stable conditions maintained during the early stages of HDT. However, after increasing the temperature, the absence of liquid yield and the formation of solids could be the reason for having no results as reported above.

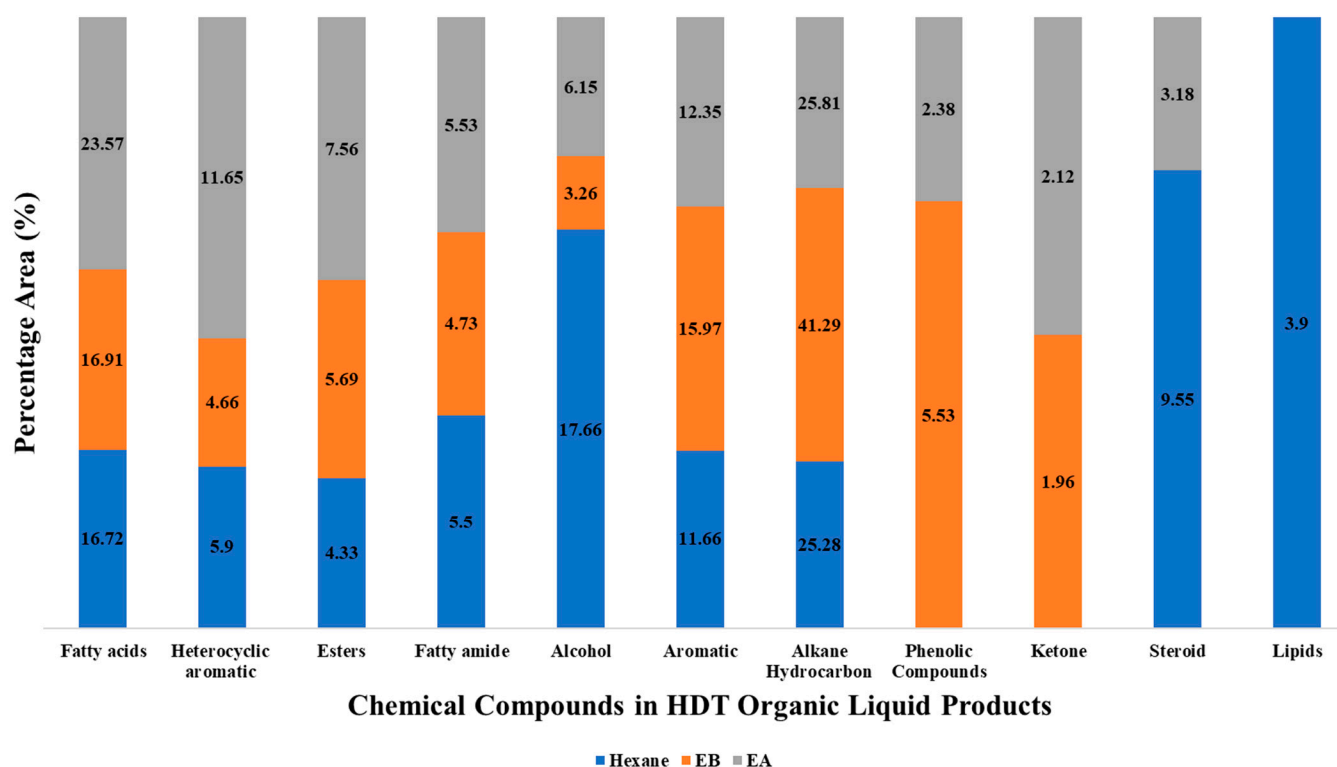


Figure 5. Chemical composition of HDT organic liquid yield products.

Chemical Compound Compositions in HDT Organic Liquid Product

The organic liquid yield from HDT at 220 °C was chosen for further analysis and GC-MS characterization due to its favorable elemental results (Table 3). Supporting materials provide comprehensive information, including total ion chromatograms (TIC) and detailed data tables with retention times and peak areas (Figures S6–S8 and Tables S6–S8), covering the HDT products of all solvent-extracted biocrude. In Figure 4, the chemical compositions are categorized by percentage area, specifically for the HDT organic phase liquid yield obtained from hexane, EB, and EA-extracted biocrude.

The results revealed a significant reduction in fatty acids concentration following the HDT treatment of hexane, EB, and EA-extracted biocrude, with decreases of 69.4%, 61.49%, and 51.6%, respectively, compared to HTL-extracted biocrude. Conversely, organic liquid products obtained from HDT exhibited an increased presence of alkane hydrocarbons, including n-alkanes and cyclo-alkanes like heptadecane and cyclooctane, with the highest concentration of 41.29% in EB, followed by 25.81% in EA and 25.28% in hexane, for all solvent-extracted biocrude after the HDT process. The reduction in fatty acids and the production of alkane hydrocarbons have a direct correlation, as reported in previous studies, where HDT of fatty acids led to alkane production via decarboxylation, decarbonylation, and hydrodeoxygenation (HDO) pathways during the upgrading process [67,70].

The possible reaction pathways for the major compound classes present in the extracted biocrudes are summarized in Figure 6. Fatty acids undergo HDO via hydrogenation to aldehydes, further reduction to alcohols, and dehydration/hydrogenation to yield alkanes. Alternatively, decarboxylation or decarbonylation can produce a one-carbon-shorter alkane with CO₂ or CO release. Fatty amides are hydrogenated to amines or alcohols, which then undergo hydrodeamination or HDO to form alkanes, releasing NH₃. N-containing heterocycles are hydrogenated, undergo ring opening where applicable, and are converted to saturated hydrocarbons via hydrodenitrogenation (HDN) with NH₃ release. O-containing heterocycles follow a similar sequence: hydrogenation to cyclic alcohols, ring opening to

linear alcohols or aldehydes, and final conversion to alkanes via HDO or dehydration. These pathways align with reported HDT mechanisms for bio-oil upgrading.

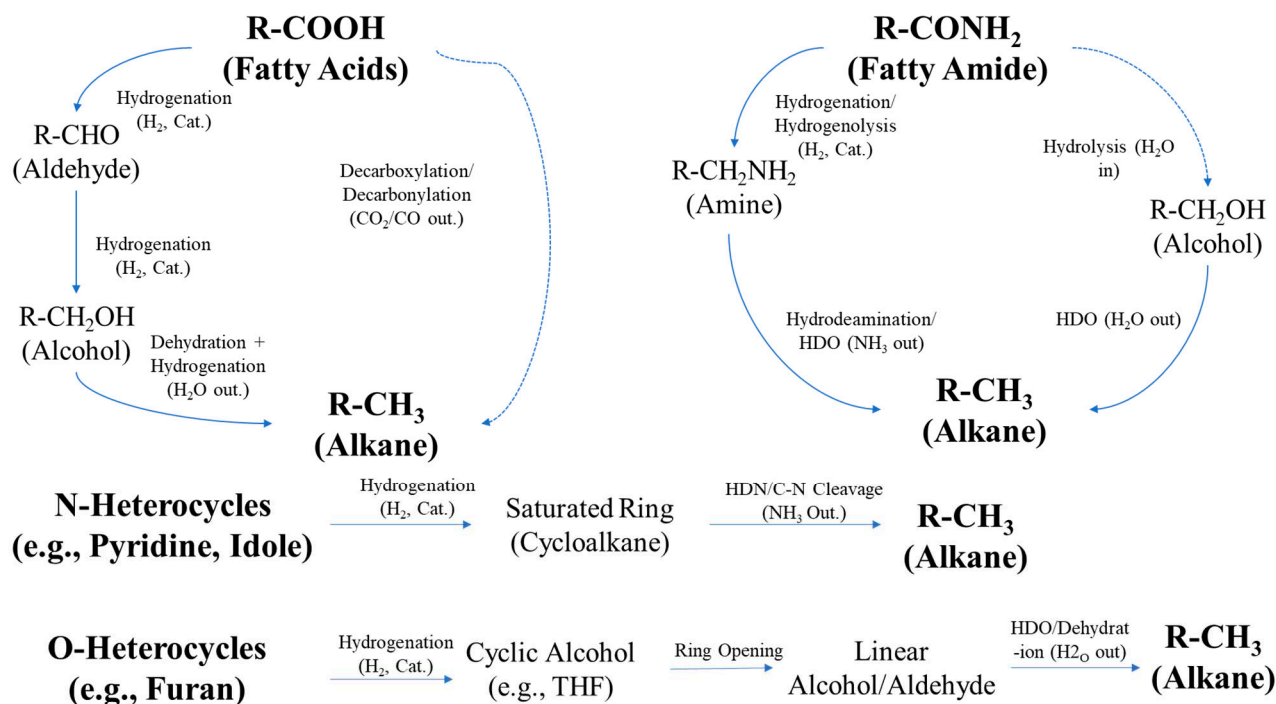


Figure 6. Proposed reaction pathways for the hydrotreatment of HTL biocrude, showing the conversion of fatty acids, amides, and heterocycles to alkanes.

Furthermore, the decrease in esters and ketones coincided with a higher alcohol concentration, such as 1-Hexadecanol in hexane, EB, and EA-extracted biocrude following HDT. This observation aligns with the findings that fatty alcohols can be obtained through the catalytic hydrogenolysis of fatty acid methyl esters [67], while alcohols are produced via the catalytic hydrogenation of ketones and aldehydes [71,72].

The decrease in heterocyclic aromatics by 42.99% in hexane, 44.56% in EB, and 21.86% in EA-extracted biocrude during HDT may result from the opening and aromatization of complex biocrude molecules. Simultaneously, the decreasing trend of N-containing (fatty amid) compounds suggests the hydro-denitrogenation of N-containing molecules [73,74].

4. Techno-Economic Comparison

Our latest work on the techno-economic and environmental performance of SS valorization routes [35] demonstrated the clear advantages of HTL with upgrading over conventional and alternative processes. Among the evaluated pathways, including HTL with upgrading, transesterification, and incineration, the HTL-upgrading route delivered the highest energy output of approximately 4,000,000 MJ/year, which is about 30% greater than that of incineration. It also achieved substantially lower greenhouse gas emissions (~700 t/year CO₂), representing nearly a 70% reduction compared to the incineration process.

From an economic perspective, HTL with upgrading achieved a net present value (NPV) of 112.9 MUS\$, far surpassing transesterification (NPV: 23.4 MUS\$), while incineration was found to be economically unviable. Sensitivity analysis revealed that even with a 50% increase in operating costs, HTL remained profitable (NPV: 62.7 MUS\$), whereas transesterification became unprofitable under the same conditions. These results underscore the economic resilience and environmental benefits of HTL with upgrading for SS

valorization. Although the present experimental study did not conduct a full Life Cycle Assessment (LCA), such an analysis is recommended in future work to provide a more comprehensive comparison with conventional approaches.

5. Limitations and Future Research Direction

This study was conducted at laboratory scale using batch reactors, and continuous operation with integrated solvent recovery was not assessed. Although solvent recycling above 95% was achieved under batch conditions, long-term stability and performance in continuous systems require further evaluation. The focus was on biocrude yield, composition, and upgrading; however, comprehensive fuel property characterization (cetane number, viscosity, density, flash point, oxidation stability) and blending performance with diesel remain to be investigated.

Advanced analyses such as FTIR, NMR, TGA/DSC, and detailed elemental profiling (Cl, P, heavy metals), along with gas composition measurements, would enable complete carbon and mass balances. Co-product streams (aqueous phase, gas, and solids) were not fully characterized, and their valorization or safe disposal strategies should be explored. While Ni/SiO₂-Al₂O₃ was selected for cost-effectiveness and proven activity, testing alternative catalysts (CoMo, NiMo, bifunctional systems) under milder conditions could reduce hydrogen consumption. Finally, pilot-scale techno-economic and Life Cycle Assessment (LCA) studies are needed to validate process scalability and benchmark against conventional fuel production routes.

6. Conclusions

This study demonstrated a comprehensive approach to optimize SS valorization through HTL, selective solvent extraction, and catalytic hydrotreatment. Biocrude yields and qualities were significantly influenced by temperature and solvent choice. Maximum yields were achieved at 350 °C, with EB and DCM producing over 50 wt% biocrude, while hexane and EA showed moderate performance due to their polarity. Elemental and energy analyses confirmed that hexane-extracted biocrude had the highest carbon content and heating value, whereas DCM-extracted biocrude retained more nitrogen due to its affinity for polar compounds.

The chemical profiling of biocrudes via GC-MS revealed fatty acids, especially palmitic acid, as the predominant fraction across all solvents, supported by high lipid content in SS. Notably, solvent polarity influenced the solubility of nitrogenous and aromatic compounds. Subsequent hydrotreatment using a cost-effective Ni/SiO₂-Al₂O₃ catalyst significantly improved fuel quality by enriching saturated hydrocarbons and reducing heteroatom content, making the upgraded biocrude more suitable for fuel applications.

Overall, the findings reinforce the importance of integrated optimization across HTL conditions, solvent extraction selectivity, and upgrading strategies. Future studies should further explore continuous-flow upgrading systems, long-term catalyst stability, and techno-economic assessments to facilitate the deployment of sludge-derived biofuels in commercial energy systems.

Supplementary Materials: The following supporting information can be downloaded at: <https://www.mdpi.com/article/10.3390/en18174568/s1>. Table S1 shows hydrothermal liquefaction (HTL) product yields at different sludge-to-water ratios and solvents. Figures S1–S8 present reactor design specifications and GC-MS chromatograms of biocrude and hydrotreated products. Tables S2–S8 provide detailed GC-MS compound compositions of solvent-extracted biocrudes (DCM, hexane, EA, EB) and their corresponding hydrotreatment products.

Author Contributions: M.U.: conceptualization, methodology, analysis and characterization and writing—original draft, S.C.: writing—review and editing, S.B.: writing—review and editing, M.A.: writing—review and editing and resources and J.S.C.: supervision, resources, writing—review and editing. All authors have read and agreed to the published version of the manuscript.

Funding: This research did not receive any specific grant from funding agencies in the public, commercial, or not-for-profit sectors.

Data Availability Statement: All data has been reported and provided in this manuscript. Further inquiries can be directed to the corresponding author.

Acknowledgments: The first author would like to acknowledge the Japan Ministry of Education, Culture, Sports, Science and Technology (MEXT) financial support for the MEXT Scholarship for graduate studies. The authors also thank Muhammad Aziz and his Lab at the University of Tokyo for providing the hydrotreatment research facility. The authors also thank Mayuko Nakagawa for providing and assisting in the GCMS characterization. In preparing this manuscript, the first author utilized generative AI tools, specifically Quillbot and ChatGPT (version 4o), to assist in rewriting, rephrasing, and checking the grammar of his original writing for clarity and readability of the content.

Conflicts of Interest: The authors affirm that they do not have any known financial interest or personal relationships that might be perceived as influencing the research presented in this paper.

References

1. Quan, C.; Kamran, K.; Williams, P.T. Thermochemical conversion of sewage sludge: A critical review. *Prog. Energy Combust. Sci.* **2020**, *79*, 100843. [CrossRef]
2. Semblante, G.U.; Hai, F.I.; Bustamante, H.; Price, W.E.; Nghiem, L.D. Effects of sludge retention time on oxic-settling-anoxic process performance: Biosolids reduction and dewatering properties. *Bioresour. Technol.* **2016**, *218*, 1187–1194. [CrossRef]
3. Seiple, T.E.; Coleman, A.M.; Skaggs, R.L. Municipal wastewater sludge as a sustainable bioresource in the United States. *J. Environ. Manag.* **2017**, *197*, 673–680. [CrossRef]
4. Syed-Hassan, S.S.A.; Wang, Y.; Hu, S.; Su, S.; Xiang, J. Thermochemical processing of sewage sludge to energy and fuel: Fundamentals, challenges and considerations. *Renew. Sustain. Energy Rev.* **2017**, *80*, 888–913. [CrossRef]
5. Mahzoun, Y. Heating Value and Energy Recovery Potential of Sewage Sludge and Suspended Solids in Municipal Wastewater Treatment Plant. Ph.D. Thesis, Kyoto University, Kyoto, Japan, 2018. [CrossRef]
6. Collivignarelli, M.C.; Abbà, A.; Frattarola, A.; Miino, M.C.; Padovani, S.; Katsoyiannis, I.A.; Torretta, V. Legislation for the reuse of biosolids on agricultural land in Europe: Overview. *Sustainability* **2019**, *11*, 6015. [CrossRef]
7. EEA, Bio-Waste in Europe—Turning Challenges Into Opportunities, European Environment Agency. 2023. Available online: <https://www.eea.europa.eu/publications/bio-waste-in-europe> (accessed on 12 October 2024).
8. Thomsen, L.B.S.; Carvalho, P.N.; Passos, J.S.D.; Anastasakis, K.; Bester, K.; Biller, P. Hydrothermal liquefaction of sewage sludge; energy considerations and fate of micropollutants during pilot scale processing. *Water Res.* **2020**, *183*, 116101. [CrossRef] [PubMed]
9. Liang, J.; Li, B.; Zhu, L.; Li, R.; Zhang, J.; Shi, X.; Li, X. Hydrothermal treatment and biorefinery of sewage sludge for waste reduction and production of fungal hyphae fibers and volatile fatty acids. *J. Clean. Prod.* **2021**, *289*, 125715. [CrossRef]
10. Ferrentino, R.; Langone, M.; Andreottola, G. Progress toward full scale application of the anaerobic side-stream reactor (ASSR) process. *Bioresour. Technol.* **2019**, *272*, 267–274. [CrossRef]
11. Elalami, D.; Carrere, H.; Monlau, F.; Abdelouahdi, K.; Oukarroum, A.; Barakat, A. Pretreatment and co-digestion of wastewater sludge for biogas production: Recent research advances and trends. *Renew. Sustain. Energy Rev.* **2019**, *114*, 109287. [CrossRef]
12. Nguyễn, V.K.; Chaudhary, D.K.; Dahal, R.H.; Trinh, N.H.; Kim, J.; Chang, S.W.; Hong, Y.; La, D.D.; Nguyen, X.C.; Ngo, H.H.; et al. Review on pretreatment techniques to improve anaerobic digestion of sewage sludge. *Fuel* **2021**, *285*, 119105. [CrossRef]
13. United Nations World Water Assessment Programme. Wastewater: The Untapped Resource—The United Nations World Water Development Report 2017; United Nations Educational, Scientific and Cultural Organization (UNESCO), on Behalf of the United Nations World Water Assessment Programme (WWAP). 2015. Available online: <https://wedocs.unep.org/20.500.11822/20448> (accessed on 25 October 2023).
14. MLIT. Ministry of Land, Infrastructure, Transport and Tourism. Systematization of Resource/Energy Recycling. MLIT. 2023. Available online: https://www.mlit.go.jp/en/mizukokudo/sewage/index_e.html (accessed on 25 October 2023).
15. Usman, M.; Cheng, S.; Cross, J.S. Biomass Feedstocks for Liquid Biofuels Production in Hawaii & Tropical Islands: A Review. *Int. J. Renew. Energy Dev.* **2021**, *11*, 111–132. [CrossRef]

16. IEA. Transport—Topics—IEA. International Energy Agency. IEA. 2021. Available online: <https://www.iea.org/topics/transport#:~:text=Transport%20has%20the%20highest%20reliance,of%20alternative%20fuels%20remains%20limited> (accessed on 18 May 2024).
17. Babayigit, E.; Alper, D.A.; Erdinçler, A. Direct Liquid–Liquid Lipid Extraction Method for Biodiesel Production from Sewage and Petrochemical Industry Sludges. *Waste Biomass Valorization* **2018**, *9*, 2471–2479. [[CrossRef](#)]
18. Usman, M. Production of Biodiesel from Wastewater Sludge Treatment by Direct Lipids Extraction. *J. Fundam. Renew. Energy Appl.* **2018**, *8*, 1000261. [[CrossRef](#)]
19. Gil, A.; Siles, J.; Martín, M.; Chica, A.; Estévez-Pastor, F.; Toro-Baptista, E. Effect of microwave pretreatment on semi-continuous anaerobic digestion of sewage sludge. *Renew. Energy* **2018**, *115*, 917–925. [[CrossRef](#)]
20. Bora, A.P.; Gupta, D.P.; Durbha, K.S. Sewage sludge to bio-fuel: A review on the sustainable approach of transforming sewage waste to alternative fuel. *Fuel* **2020**, *259*, 116262. [[CrossRef](#)]
21. Jahromi, H.; Adhikari, S.; Roy, P.; Hassani, E.; Pope, C.; Oh, T.-S.; Karki, Y. Production of green transportation fuels from Brassica carinata oil: A comparative study of noble and transition metal catalysts. *Fuel Process. Technol.* **2021**, *215*, 106737. [[CrossRef](#)]
22. Wang, G.; Zhang, J.; Yu, J.; Zhu, Z.; Guo, X.; Chen, G.; Pedersen, T.H.; Rosendahl, L.; Yu, X.; Wang, H. Catalytic hydrothermal liquefaction of sewage sludge over alumina-based and attapulgite-based heterogeneous catalysts. *Fuel* **2022**, *323*, 124329. [[CrossRef](#)]
23. Ghodke, P.K.; Sharma, A.K.; Pandey, J.; Chen, W.; Patel, A.; Ashokkumar, V. Pyrolysis of sewage sludge for sustainable biofuels and value-added biochar production. *J. Environ. Manag.* **2021**, *298*, 113450. [[CrossRef](#)]
24. Sahoo, A.K.; Saini, K.; Jindal, M.; Bhaskar, T.; Pant, K.K. Co-Hydrothermal Liquefaction of algal and lignocellulosic biomass: Status and perspectives. *Bioresour. Technol.* **2021**, *342*, 125948. [[CrossRef](#)]
25. Usman, M.; Cheng, S.; Boonyubol, S.; Cross, J.S. The future of aviation soars with HTL-based SAFs: Exploring potential and overcoming challenges using organic wet feedstocks. *Sustain. Energy Fuels* **2023**, *7*, 4066–4087. [[CrossRef](#)]
26. Usman, M.; Cheng, S.; Boonyubol, S.; Cross, J.S. From biomass to biocrude: Innovations in hydrothermal liquefaction and upgrading. *Energy Convers. Manag.* **2024**, *302*, 118093. [[CrossRef](#)]
27. Watson, J.; Lu, J.; De Souza, R.; Si, B.; Zhang, Y.; Liu, Z. Effects of the extraction solvents in hydrothermal liquefaction processes: Biocrude oil quality and energy conversion efficiency. *Energy* **2018**, *167*, 189–197. [[CrossRef](#)]
28. Jahromi, H.; Rahman, T.; Roy, P.; Adhikari, S. Hydrotreatment of solvent-extracted biocrude from hydrothermal liquefaction of municipal sewage sludge. *Energy Convers. Manag.* **2022**, *263*, 115719. [[CrossRef](#)]
29. Rahman, T.; Jahromi, H.; Roy, P.; Adhikari, S.; Hassani, E.; Oh, T.-S. Hydrothermal liquefaction of municipal sewage sludge: Effect of red mud catalyst in ethylene and inert ambiances. *Energy Convers. Manag.* **2021**, *245*, 114615. [[CrossRef](#)]
30. Kilgore, U.; Diaz, E.; Spry, B.; Jiang, Y.; Li, S.; Schmidt, A.; Thorson, M.R. Solvent processing for improved separation of hydrothermal liquefaction products. *Sustain. Energy Fuels* **2024**, *8*, 3279–3289. [[CrossRef](#)]
31. Usman, M.; Cheng, S.; Boonyubol, S.; Cross, J.S. Evaluating Green Solvents for Bio-Oil Extraction: Advancements, challenges, and future perspectives. *Energies* **2023**, *16*, 5852. [[CrossRef](#)]
32. De Jesus, S.S.; Filho, R.M. Recent advances in lipid extraction using green solvents. *Renew. Sustain. Energy Rev.* **2020**, *133*, 110289. [[CrossRef](#)]
33. Janicka, P.; Płotka-Wasyłka, J.; Jatkowska, N.; Chabowska, A.; Fares, M.Y.; Andruch, V.; Kaykhaii, M.; Gębicki, J. Trends in the new generation of green solvents in extraction processes. *Curr. Opin. Green Sustain. Chem.* **2022**, *37*, 100670. [[CrossRef](#)]
34. Usman, M.; Cheng, S.; Boonyubol, S.; Cross, J.S. Nitrogen Minimization in Hydrothermal Liquefaction Biocrude from Sewage Sludge with Green Extraction Solvents. *ACS Omega* **2024**, *9*, 14530–14538. [[CrossRef](#)]
35. Usman, M. Techno-Economic and Emissions Comparison of Waste-to-Fuel via Hydrothermal Liquefaction, Transesterification, and Incineration. *J. Econ. Technol.* **2024**, *3*, 237–250. [[CrossRef](#)]
36. Oh, S.; Hwang, H.; Choi, H.S.; Choi, J.W. The effects of noble metal catalysts on the bio-oil quality during the hydrodeoxygenative upgrading process. *Fuel* **2015**, *153*, 535–543. [[CrossRef](#)]
37. Lee, E.H.; Park, R.-S.; Kim, H.; Park, S.; Jung, S.; Jeon, J.; Kim, S.C.; Park, Y.-K. Hydrodeoxygenation of guaiacol over Pt loaded zeolitic materials. *J. Ind. Eng. Chem.* **2016**, *37*, 18–21. [[CrossRef](#)]
38. Jahromi, H.; Agblevor, F.A. Upgrading of pinyon-juniper catalytic pyrolysis oil via hydrodeoxygenation. *Energy* **2017**, *141*, 2186–2195. [[CrossRef](#)]
39. Niaounakis, M. Treatments and Uses. In *Management of Marine Plastic Debris*; Elsevier: Amsterdam, The Netherlands, 2017; pp. 215–315. [[CrossRef](#)]
40. Fan, Y.; Hornung, U.; Dahmen, N. Hydrothermal liquefaction of sewage sludge for biofuel application: A review on fundamentals, current challenges and strategies. *Biomass Bioenergy* **2022**, *165*, 106570. [[CrossRef](#)]
41. Li, B.; Song, H.; Yang, T.; Liu, E.; Li, R. Hydrothermal liquefaction of sewage sludge and model compound: Heavy metals distribution and behaviors. *J. Anal. Appl. Pyrolysis* **2023**, *169*, 105800. [[CrossRef](#)]

42. Xu, D.; Lin, G.; Liu, L.; Wang, Y.; Jing, Z.; Wang, S. Comprehensive evaluation on product characteristics of fast hydrothermal liquefaction of sewage sludge at different temperatures. *Energy* **2018**, *159*, 686–695. [[CrossRef](#)]
43. Villaver, W.S.; Carpio, R.B.; Yap, K.J.R.; De Leon, R.L. Effects of temperature and reaction time on yield and properties of biocrude oil produced by hydrothermal liquefaction of *Spirulina platensis*. *Int. J. Smart Grid Clean Energy* **2018**, *7*, 32–41. [[CrossRef](#)]
44. Shah, A.A.; Toor, S.; Conti, F.; Nielsen, A.H.; Rosendahl, L. Hydrothermal liquefaction of high ash containing sewage sludge at sub and supercritical conditions. *Biomass Bioenergy* **2020**, *135*, 105504. [[CrossRef](#)]
45. Seehar, T.H.; Toor, S.; Sharma, K.; Nielsen, A.H.; Pedersen, T.H.; Rosendahl, L. Influence of process conditions on hydrothermal liquefaction of eucalyptus biomass for biocrude production and investigation of the inorganics distribution. *Sustain. Energy Fuels* **2021**, *5*, 1477–1487. [[CrossRef](#)]
46. De Souza Costa, P.; Mata, R.A.; Pinto, M.F.; Paradela, F.; Dutra, F.R. Hydrothermal liquefaction of microalgae for the production of biocrude and value-added chemicals. *Chem. Eng. Trans.* **2022**, *94*, 865–870. [[CrossRef](#)]
47. Xue, Y.; Chen, H.; Zhao, W.; Yang, C.; Ma, P.; Han, S. A review on the operating conditions of producing bio-oil from hydrothermal liquefaction of biomass. *Int. J. Energy Res.* **2016**, *40*, 865–877. [[CrossRef](#)]
48. Bayat, H.; Dehghanizadeh, M.; Jarvis, J.M.; Brewer, C.E.; Jena, U. Hydrothermal liquefaction of food waste: Effect of process parameters on product yields and chemistry. *Front. Sustain. Food Syst.* **2021**, *5*, 658592. [[CrossRef](#)]
49. Cravotto, C.; Fabiano-Tixier, A.-S.; Claux, O.; Abert-Vian, M.; Tabasso, S.; Cravotto, G.; Chemat, F. Towards Substitution of Hexane as Extraction Solvent of Food Products and Ingredients with No Regrets. *Foods* **2022**, *11*, 3412. [[CrossRef](#)]
50. Comandella, D.; Bignami, M.; Fürst, P.; Grob, K.; Mengelers, M.; Cascio, C.; Xiftou, K.; Croera, C.; Lambré, C. Technical Report on the Need for Re-Evaluation of the Safety of Hexane Used as an Extraction Solvent in the Production of Foodstuffs and Food Ingredients. *EFSA Support. Publ.* **2024**, *21*, 9001E. [[CrossRef](#)]
51. Groß, P.; Ihmels, H. Studies about the Effect of Halogenated Solvents on the Fluorescence Properties of 9-Aryl-Substituted Isoquinolinium Derivatives—A Case Study. *J. Fluoresc.* **2024**, *35*, 2407–2414. [[CrossRef](#)]
52. Carré, P.; Berthold, S.; Piofczyk, T.; Bothe, S.; Hadjiali, S. Solvent Solutions: Comparing Extraction Methods for Edible Oils and Proteins in a Changing Regulatory Landscape. Part 1: Physical-Properties. *OCL* **2024**, *31*, 12. [[CrossRef](#)]
53. Badawy, T.; Williamson, J.; Xu, H. Laminar Burning Characteristics of Ethyl Propionate, Ethyl Butyrate, Ethyl Acetate, Gasoline and Ethanol Fuels. *Fuel* **2016**, *183*, 627–640. [[CrossRef](#)]
54. Byrne, F.P.; Forier, B.; Bossaert, G.; Hoebbers, C.; Farmer, T.J.; Hunt, A.J. A Methodical Selection Process for the Development of Ketones and Esters as Bio-Based Replacements for Traditional Hydrocarbon Solvents. *Green Chem.* **2018**, *20*, 4003–4011. [[CrossRef](#)]
55. Usman, M.; Cheng, S.; Cross, J.S. Biodiesel production from urban and suburban municipal sewage sludges in Tokyo, Japan. In Proceedings of the International Conference and Utility Exhibition on Energy, Environment and Climate Change (ICUE 2022), Pattaya, Thailand, 26–28 October 2022. [[CrossRef](#)]
56. Usman, M.; Cheng, S.; Cross, J.S. Biodiesel production from wet sewage sludge and reduced CO₂ emissions compared to incineration in Tokyo, Japan. *Fuel* **2023**, *341*, 127614. [[CrossRef](#)]
57. Chen, Y.; Mu, R.; Yang, M.; Fang, L.; Wu, Y.; Wu, K.; Ya, L.; Gong, J. Catalytic hydrothermal liquefaction for bio-oil production over CNTs supported metal catalysts. *Chem. Eng. Sci.* **2017**, *161*, 299–307. [[CrossRef](#)]
58. Wang, F.; Shen, H.; Liu, T.; Yang, X.; Yang, Y.; Guo, Y. Formation of pyrazines in Maillard model systems: Effects of structures of Lysine-Containing Dipeptides/Tripeptides. *Foods* **2021**, *10*, 273. [[CrossRef](#)]
59. Kłosowski, G.; Mikulski, D.; Pielech-Przybylska, K. Pyrazines Biosynthesis by *Bacillus* Strains Isolated from Natto Fermented Soybean. *Biomolecules* **2021**, *11*, 1736. [[CrossRef](#)]
60. Zhu, Z.; Toor, S.; Rosendahl, L.; Yu, D.; Chen, G. Influence of alkali catalyst on product yield and properties via hydrothermal liquefaction of barley straw. *Energy* **2015**, *80*, 284–292. [[CrossRef](#)]
61. Luo, L.; Dai, L.; Savage, P.E. Catalytic hydrothermal liquefaction of soy protein concentrate. *Energy Fuels* **2015**, *29*, 3208–3214. [[CrossRef](#)]
62. Zhang, Z.; Zhou, Y.; Zhang, J.; Xia, S.; Hermanowicz, S.W. Effects of short-time aerobic digestion on extracellular polymeric substances and sludge features of waste activated sludge. *Chem. Eng. J.* **2016**, *299*, 177–183. [[CrossRef](#)]
63. Nie, E.; Zheng, G.; Gao, D.; Chen, T.; Yang, J.; Wang, Y.; Wang, X. Emission characteristics of VOCs and potential ozone formation from a full-scale sewage sludge composting plant. *Sci. Total Environ.* **2019**, *659*, 664–672. [[CrossRef](#)]
64. Masyita, A.; Sari, R.M.; Astuti, A.D.; Yasir, B.; Rumata, N.R.; Emran, T.B.; Nainu, F.; Simal-Gándara, J. Terpenes and terpenoids as main bioactive compounds of essential oils, their roles in human health and potential application as natural food preservatives. *Food Chem. X* **2022**, *13*, 100217. [[CrossRef](#)]
65. Golubev, O.V.; Egazar'yants, S.V.; Matevosyan, D.V.; Naranov, E.R.; Maksimov, A.L.; Karakhanov, E.A. Development of Protective-Layer Catalysts for Removal of Chlorine Compounds from Diesel Fractions. *Russ. J. Appl. Chem.* **2018**, *91*, 2040–2045. [[CrossRef](#)]
66. Mitra, S.; Sulakhe, S.; Shown, B.; Mandal, S.; Das, A. Organic chlorides in petroleum crude oil: Challenges for refinery and mitigations. *ChemBioEng Rev.* **2022**, *9*, 319–332. [[CrossRef](#)]

67. Gandarias, I.; Arias, P.L. Hydrotreating catalytic processes for oxygen removal in the upgrading of Bio-Oils and Bio-Chemicals. In *Liquid, Gaseous and Solid Biofuels—Conversion Techniques*; InTech eBooks: Rijeka, Croatia, 2013. [CrossRef]
68. Rogers, K.; Zheng, Y. Selective Deoxygenation of Biomass-Derived Bio-oils within Hydrogen-Modest Environments: A Review and New Insights. *ChemSusChem* **2016**, *9*, 1750–1772. [CrossRef]
69. Zhang, S.; Liu, X.; Xu, Y.; Tang, Y. Temperature-Dependent hydrogenation, hydrodeoxygenation, and hydrogenolysis of anisole on nickel catalysts. *Catalysts* **2023**, *13*, 1418. [CrossRef]
70. Mussa, N.-S.; Toshtay, K.; Capron, M. Catalytic Applications in the production of hydrotreated Vegetable Oil (HVO) as a renewable fuel: A review. *Catalysts* **2024**, *14*, 452. [CrossRef]
71. CHEM, Libretexts, 1.7: 1.7-Chemical properties III- Catalytic Hydrogenation. Chemistry LibreTexts, 2017. Available online: https://chem.libretexts.org/Courses/Brevard_College/CHE_202%3A_Organic_Chemistry_II/01%3A_Aldehydes_and_Ketones/1.07%3A_1.7-Chemical_properties_III-_Catalytic_Hydrogenation#:~:text=The%20simplest%20large%2Dscale%20procedure,The%20product%20is%20an%20alcohol (accessed on 23 September 2024).
72. Witsuthammakul, A.; Sooknoi, T. Selective hydrodeoxygenation of bio-oil derived products: Ketones to olefins. *Catal. Sci. Technol.* **2015**, *5*, 3639–3648. [CrossRef]
73. He, Z.; Xu, H.; Zhou, C.; Xin, Z.; Liu, J.; Shen, B. A kinetic model for in situ coking denitrification of heavy oil with high nitrogen content based on starch using a structure-oriented lumping method. *RSC Adv.* **2018**, *8*, 32707–32718. [CrossRef]
74. Hu, Y.; Li, J.; Wang, S.; Xu, L.; Barati, B.; Cao, B.; Wang, H.; Xie, K.; Wang, Q. Catalytic fast hydrolysis of seaweed biomass with different zeolite catalysts to produce high-grade bio-oil. *Process Saf. Environ. Prot.* **2021**, *146*, 69–76. [CrossRef]

Disclaimer/Publisher’s Note: The statements, opinions and data contained in all publications are solely those of the individual author(s) and contributor(s) and not of MDPI and/or the editor(s). MDPI and/or the editor(s) disclaim responsibility for any injury to people or property resulting from any ideas, methods, instructions or products referred to in the content.